

Are we using appropriate segmentation metrics? Identifying correlates of human expert perception for CNN training beyond rolling the DICE coefficient

Florian Kofler^{1,7,8}, Ivan Ezhov^{1,8}, Fabian Isensee², Fabian Balsiger³, Christoph Berger¹, Maximilian Koerner¹, Johannes Paetzold^{1,8}, Hongwei Li^{1,10}, Suprosanna Shit^{1,8}, Richard McKinley³, Spyridon Bakas^{4,5,6}, Claus Zimmer⁷, Donna Ankerst⁹, Jan Kirschke^{7,8}, Benedikt Wiestler^{7,8*}, and Bjoern H. Menze^{1,10*}

¹ Department of Informatics, Technical University Munich, Germany

² HIP Applied Computer Vision Lab, Division of Medical Image Computing, German Cancer Research Center (DKFZ), Germany

³ Support Center for Advanced Neuroimaging (SCAN), Institute for Diagnostic and Interventional Neuroradiology, Inselspital, Bern University Hospital, University of Bern, Switzerland

⁴ Center for Biomedical Image Computing and Analytics (CBICA), University of Pennsylvania, USA

⁵ Department of Radiology, Perelman School of Medicine, University of Pennsylvania, USA

⁶ Department of Pathology and Laboratory Medicine, Perelman School of Medicine, University of Pennsylvania, USA

⁷ Department of Diagnostic and Interventional Neuroradiology, School of Medicine, Klinikum rechts der Isar, Technical University of Munich, Germany

⁸ TranslaTUM - Central Institute for Translational Cancer Research, Technical University of Munich, Germany

⁹ Depts of Mathematics and Life Science Systems, Technical University of Munich, Germany

¹⁰ Department of Quantitative Biomedicine, University of Zurich, Switzerland
{florian.kofler}@tum.de

Abstract. In this study, we explore quantitative correlates of qualitative human expert perception. We discover that current quality metrics and loss functions, considered for biomedical image segmentation tasks, correlate moderately with segmentation quality assessment by experts, especially for small yet clinically relevant structures, such as the enhancing tumor in brain glioma. We propose a method employing classical statistics and experimental psychology to create complementary compound loss functions for modern deep learning methods, towards achieving a better fit with human quality assessment. When training a CNN for delineating adult brain tumor in MR images, all four proposed loss

* contributed equally as senior authors

candidates outperform the established baselines on the clinically important and hardest to segment enhancing tumor label, while maintaining performance for other label channels.

1 Introduction

In the medical imaging community challenges have become a prominent forum to benchmark segmentation performance of the latest methodological advances [1,2,3,4]. Across all challenges, convolutional neural networks (CNNs), and in particular the U-Net architecture [5], gained increasing popularity over the years. Typically, segmentation models are evaluated (and trained) using well-established criteria, such as the Dice similarity coefficient or the Hausdorff distance, or combinations thereof. Segmentation models for the BraTS challenge [4] for example are typically trained and evaluated on three label channels: *enhancing tumor (ET)*, *tumor core (TC)* and *whole tumor (WT)* compartments. For the final ranking in the BraTS challenge these three channels are treated equally. In contrast, from a medical perspective, the ET channel is of higher importance, as in glioma surgery, gross total resection of the ET is aimed for [6] and tumor progression is mainly defined by an increase in ET volume [7].

Like BraTS, most challenges rely upon a combination of Dice coefficient (DICE) with other metrics [8] for their scoring [1]. However, it is not well understood and investigated how such metrics reflect expert opinion on segmentation quality and clinical relevance. Taha et al. [9] investigated how different aspects of segmentation quality are captured by different metrics. Despite the central importance of segmentation metrics for evaluation of segmentation performance, there is a clear gap in knowledge how to best capture expert assessment of a "good" (clinically meaningful) segmentation. This problem arises especially when selecting a loss function for CNN training. In contrast to a plethora of volumetric loss functions [10,11,12,13,14,15], only few non-volumetric losses are established for CNN training such as [16]¹¹.

Our contribution to the field is multifaceted. First, our study develops a better understanding of the qualitative human expert assessment in the example of glioma image analysis by identifying its quantitative correlates. Building upon these insights, we propose a method exploiting techniques of classical statistics and experimental psychology to form new compound losses for modern neural network training. These losses achieve a better fit with human quality assessment and improve on conventional baselines.

¹¹ This is especially true, when searching for multi-class segmentation losses, which support GPU-based training. For instance according to the authors there is no implementation of [16] with GPU support.

2 Methods

2.1 Collection of expert ratings

To understand how expert radiologists assess the quality of tumor segmentations, we conduct experiments where participants rate segmentation quality on a six-degree Likert scale (see Fig. 1). The selection options range from one star for *strong rejection*, to six stars for *perfect* segmentations.

Experiment 1: We randomly select three exams from eight institutions that provided data to the BraTS 2019 [1] test set. We also present one additional exam with apparently erroneous segmentation labels to check whether participants follow the instructions. We display stimulus material according to four experimental conditions, i.e. four different segmentation labels for each exam: the ground truth segmentations, segmentations from team *zyx* [17], a *SIMPLE* [18] fusion of seven segmentations [17,19,20,21,22,23,24] obtained from BraTS-Toolkit [25], and a segmentation randomly selected without replacement from all the teams participating in BraTS 2019. This results in a total of 300 trials that are presented to each expert radiologist.

Experiment 2: Experts evaluate only the axial views of the gliomas’ center of mass, on a random sample of 50 patients from our test set. We present our four candidate losses vs. the *ground truth* and *DICE+BCE* baseline as conditions, so the experiment incorporates again 300 trials.

2.2 Metrics and losses vs. qualitative expert assessment

Metrics: For each experimental condition, we compute a comprehensive set of segmentation quality metrics comparing the segmentation to the expert annotated ground truth, inspired by [9]. The metrics are calculated for the BraTS evaluation criteria: *WT*, *TC*, and *ET*, as well as the individual labels *necrosis* and *edema*. In addition, we compute mean aggregates for BraTS and individual labels, Fig. 4A. Computation of metrics is implemented using *pymia* [27].

Losses: We use the binary labels to compute established segmentation losses between the candidate segmentations and the *ground truth (GT)* following the same evaluation criteria¹². The losses we considered¹³ are shown in Table 1.

¹² To test the validity of this approach we conduct a supportive experiment, comparing *binary* segmentations to *non-binary* network outputs and achieve comparable results across all loss functions.

¹³ For Tversky loss we choose combinations which have proven successful for similar segmentation problems, parameters for α and β are written behind the code name.

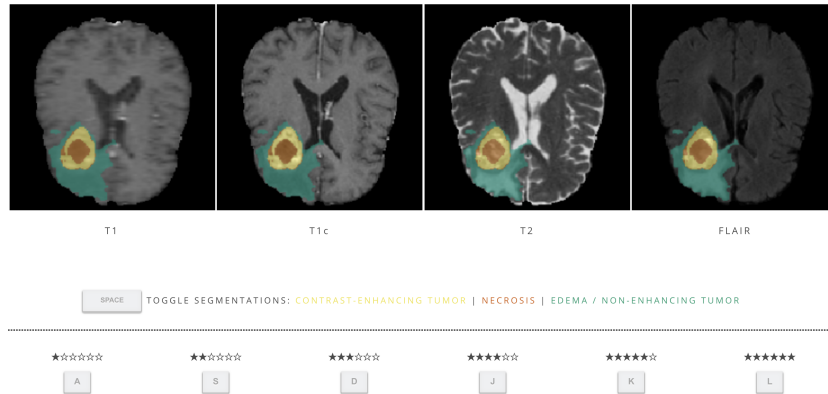


Fig. 1. Stimulus material presented to the participants implemented via *JS Psych* [26]. One trial consisted of presentation of an MR exam in either axial, sagittal or coronal view, along with the controls for the quality rating and a legend for the segmentation labels. We presented the glioma’s center of mass according to the TC, defined by the *necrosis and enhancing tumor* voxels in 2D slices of T1, T1c, T2, T2 FLAIR in a horizontal row arrangement. The stimulus presentation is conducted in line with best practices in experimental psychology (details are outlined in supplementary materials).

2.3 Construction of compound losses

We aim to design a loss function, combining complementary loss functions, to achieve a better correlation with human segmentation quality assessment. Our compound loss is structured as a weighted linear combination of losses per label channel:

$$L = \sum_i \alpha_i \sum_j w_{ij} loss_{ij} \quad (1)$$

where α_i denotes weights per channel, and w_{ij} denotes weights per loss.

Table 1. Losses considered in our analysis. Implementations are Github links.

Loss name	Loss abbreviation	Implementation	Reference
Asymmetric	ASYM	junma	[10]
Binary cross-entropy	BCE	pytorch	n/a
Dice	DICE	monai	[11]
Generalized Dice	GDICE_L	liviaets	[12]
Generalized Dice	GDICE_W	wolny	[12]
Generalized Dice	GDICE_M	monai	[12]
Hausdorff DT	HDDT	patryg	[16]
Hausdorff ER	HDER	patryg	[16]
Jaccard	IOU	junma	[13]
Jaccard	JAC	monai	[11]
Sensitivity-Specificity	SS	junma	[14]
Soft Dice	SOFTD	nnUNet	[28]
Tversky	TVERSKY	monai	[15]

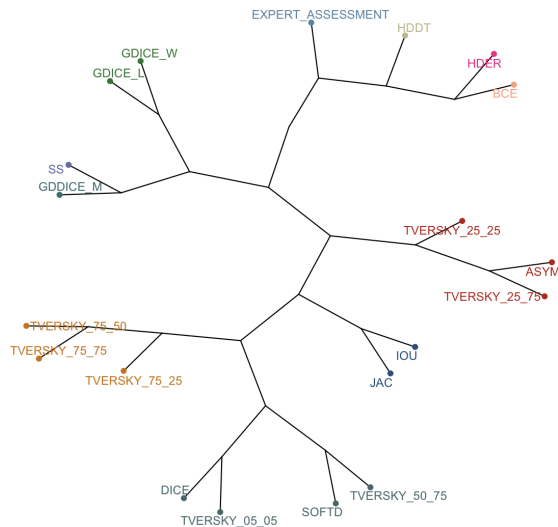


Fig. 2. Phylogenetic tree of a hierarchical clustering on an Euclidean distance matrix. Losses are colored according to ten cluster groups. We included the expert assessment for reference, one can observe how it resides somewhere between the distance based losses and the group of generalized Dice losses and SS loss. We obtain comparable findings from a *Principal Component Analysis (PCA)*, see supplemental materials.

Identifying promising loss combinations: Losses produce different signals (gradients) when they react to input signals (network outputs). With hierarchical clustering we analyze similarity in loss response patterns, see Fig. 2. We can now build complementary loss combinations by selecting elements from the different cluster groups.

Obtaining weights from the linear mixed model: Second, we evaluate the predictive performance of our combinations through linear mixed models using the *lme4* package [29]. We average the human expert rating across views to obtain a *quasi-metric* variable¹⁴. We then model the human expert assessment as a dependent variable and predict it by plugging in the loss values of our candidate combinations as predictor variables. Mixed models allow to account for the *non-independence* of data points by modelling *exam* and *experimental condition* as random factors. To identify loss candidates for CNN training, we evaluate the predictive power of our models by computing Pseudo R^2 [30], while monitoring typical mixed regression model criteria such as multi-collinearity, non-normality of residuals and outliers, homoscedasticity, homogeneity of variance and normality of random effects.

¹⁴ We deem this approach valid, as the distribution is consistent across views. See supplemental material.

2.4 CNN training

We train nnU-Net [31] using a standard BraTS trainer [32] with a moderate augmentation pipeline on the *fold 0 split* of the *BraTS 2020* training set, using the rest of the training set for validation. The official *BraTS 2020* validation set is used for testing. Apart from replacing the default *DICE+BCE* loss with our custom-tailored loss candidates, and in some cases necessary learning rate adjustments, we keep all training parameters constant¹⁵.

3 Results

3.1 Qualitative assessment vs. quantitative performance measures

A total of $n=15$ radiologists from *six* institutions took part in our first segmentation quality assessment experiment. Participants had an average experience of 10.0 ± 5.1 working years as radiologists. Fig. 3 depicts how experts evaluated the segmentation quality. Next, we explore how the human expert assessment correlates with quantitative measures of segmentation performance.

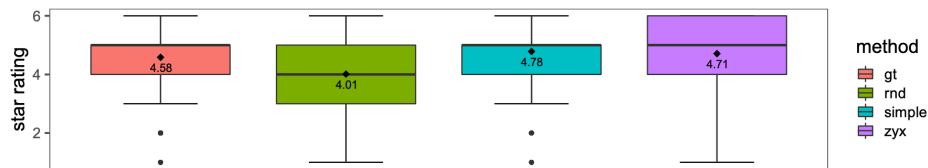


Fig. 3. Expert assessment in star rating. Diamonds indicate mean scores. Expert radiologists rated the *simple* fusion, slightly higher than the best individual docker algorithm *zyx*. The fusions’ mean improvement is mainly driven by more robust segmentation performance with less outliers towards the bottom, interestingly this effect is partially compensated by minor imperfections. We observe that both of these algorithmic segmentations receive slightly higher scores than the human expert annotated *ground truth* (*gt*). The quality of the randomly selected BraTS submissions (*rnd*) still lags behind.

Segmentation metrics vs. expert assessment: Fig. 4 depicts the Pearson correlation matrix between segmentation quality metrics and the expert assessment. We find only low to moderate correlations across all metrics, correlations are especially low for the clinically important *enhancing tumor* label. It is important to note that DICE is outperformed by other less established metrics.

¹⁵ The code for our nnU-net training will be publicly available on Github

Segmentation losses vs. expert assessment: Next we look into how these findings translate into CNN training. To train a CNN with stochastic gradient descent (SGD) a differentiable loss function is required. As this property does not apply to all metrics, we investigate how established loss functions correlate with expert quality assessment, the results are presented in Fig. 4B.

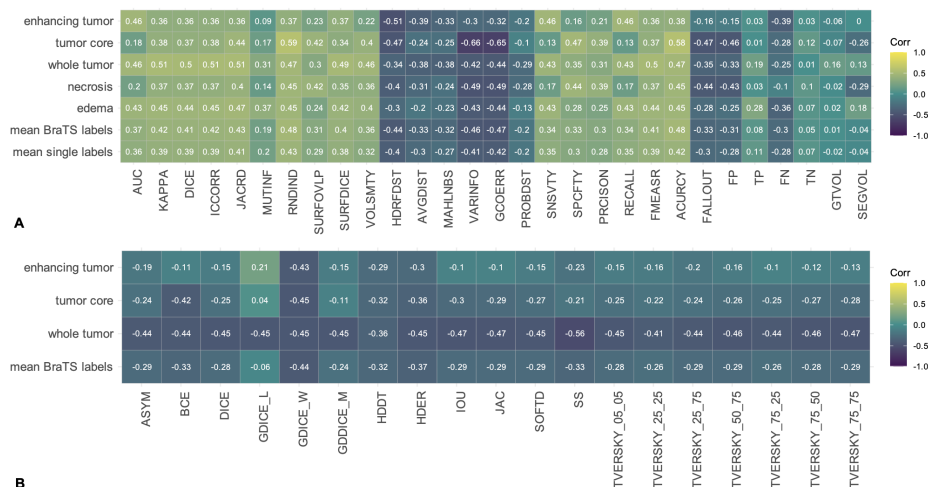


Fig. 4. A: Pearson correlation matrix: Expert assessment vs. segmentation quality metrics. The rows show the correlations for the individual label channels. In addition we present the mean aggregates for the BraTS labels (*enhancing tumor*, *tumor core* and *whole tumor*), as well as the single channels (*enhancing tumor*, *necrosis* and *edema*). For the abbreviations in the figure refer to [9,27].

B: Pearson correlation matrix: Expert assessment vs. segmentation losses. With the exception of one Generalized Dice Score implementation we observe only low correlations for the enhancing tumor and tumor core channel. In contrast multiple losses are moderately correlated for the whole tumor channel. While the IOU and JAC implementations provide very similar signals as expected, we observe huge variance across the implementations of GDICE.

3.2 Performance evaluation

Our methodology allows generating a variety of loss candidates. To evaluate the performance of our approach we obtain four promising loss candidates.

Construction of four loss candidates The first two candidates use the same combination across all label channels. Candidate *gdice.bce* uses *GDICE_W* in combination with *BCE*. Candidate *gdice.ss.bce* iterates upon this by adding *SS* loss to the equation. In contrast the candidates *channel-wise-weighted* and

channel_wise use different losses per channel: Channel *whole tumor* uses the *gdice_ss_bce* candidate loss, while channel *tumor core* is computed via the *gdice_bce* variant. In contrast the *enhancing tumor* channel relies solely on *GDICE_W*, as this is the only loss candidate with at least moderate correlation with expert assessment, compare Fig. 4B. While candidate *channel_wise* treats all channels equally the weighted variant prioritizes the more clinically relevant *tumor core* and *enhancing tumor* channels by a factor of *five*.

Evaluation of the loss candidates As depicted in Fig. 5, our loss candidates outperform the established *Dice* and *Dice+BCE* losses with regard to the clinically most important *enhancing tumor* label while maintaining performance for the *tumor core* and *whole tumor* channel. This finding is also supported by a second qualitative experiment, where three expert radiologists from two institutions detect a subtle improvement in segmentation quality (see Fig. 6).

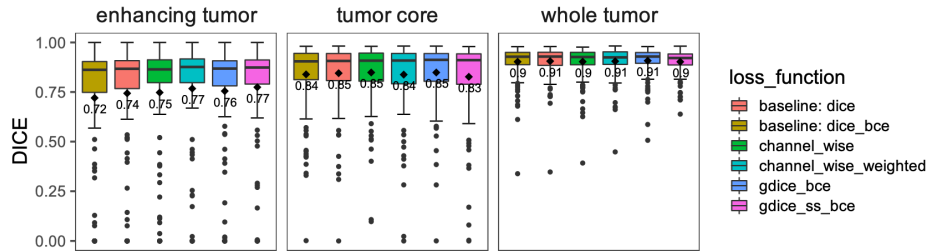


Fig. 5. Dice comparison of loss candidates vs. baselines across BraTS label channels. Diamonds indicate mean scores. P-values for paired-samples T-tests comparing our candidates with the *dice_bce* baseline from left to right: 0.1547 , 0.04642 , 0.05958 , 0.01881 for the 95% significance level. While not all t-tests generate significant *p-values* on our small test set, it is important to note that the achieved improvement is bigger than the training variance, see supplemental materials.

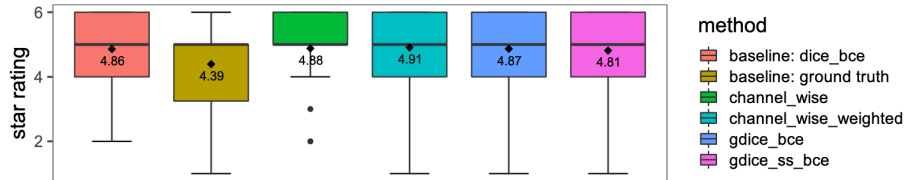


Fig. 6. Expert assessment of the four loss candidates vs ground truth and the *DICE+BCE* baseline. Diamonds indicate mean scores. We observe only subtle differences in expert rating between the *DICE+BCE* baseline and our candidates. Like in experiment 1 the human annotated ground truth is rated worse, compare Fig. 3

4 Discussion

Existing literature [33,8] reported on the discrepancy between expert segmentation quality assessment and established segmentation quality metrics. Our approach combining methods of experimental psychology and classical statistics identifies the quantitative correlates of qualitative human expert perception to shed more light on this complex phenomenon. While both entities, *segmentation quality metrics* and *expert radiologists* try to measure segmentation quality, their signals correlate only moderately, especially for *enhancing tumor (ET)*.

Even though our training set is small and the 15 radiologists judge the complex 3D segmentations on three 2D views, our method manages to extract the signal. When training a modern convolutional neural network with our expert inspired loss functions, all four proposed candidates lead to quantitative improvement on the *ET* channel, outperforming established baselines. This is in line with our expectations as the *ET* channel is of high clinical relevance for human experts.

We find that *BCE* is one of the few loss functions complementary to volumetric losses, which might explain why the empirically found *Dice+BCE* provides a solid baseline across many segmentation tasks. Our findings question the status of Dice coefficient as the *de facto gold standard* for measuring glioma segmentation quality.¹⁶ We highlight the need for development of new segmentation metrics and losses that better correlate with expert assessment. As primate perception follows a fixed, partially understood, set of rules e.g. [34,35] we speculate that our loss generation approach might generalize well to other segmentation problems, however further research is required to explore this.

5 Acknowledgments

Bjoern Menze, Benedikt Wiestler and Florian Kofler are supported through the SFB 824, subproject B12.

Supported by Deutsche Forschungsgemeinschaft (DFG) through TUM International Graduate School of Science and Engineering (IGSSE), GSC 81.

With the support of the Technical University of Munich – Institute for Advanced Study, funded by the German Excellence Initiative.

J.C. Paetzold is supported by the Graduate School of Bioengineering, Technical University of Munich.

Research reported in this publication was partly supported by the National Cancer Institute (NCI) and the National Institute of Neurological Disorders and

¹⁶ As experts consistently scored CNN segmentations higher than the human annotated ground truth in our experiments (see Fig. 3, 6), our findings raise the question whether segmentation performance in general and challenge rankings in particular should be determined based upon Dice similarity with the latter. This phenomenon might occur as humans, in contrast to machines, are prone to random errors.

Stroke (NINDS) of the National Institutes of Health (NIH), under award numbers NCI:U01CA242871, NCI:U24CA189523, NINDS:R01NS042645. The content of this publication is solely the responsibility of the authors and does not represent the official views of the NIH.

Part of this work was funded by the Helmholtz Imaging Platform (HIP), a platform of the Helmholtz Incubator on Information and Data Science.

I. Ezhov and S. Shit are supported by the Translational Brain Imaging Training Network under the EU Marie Skłodowska-Curie programme (Grant ID: 765148).

References

1. Menze, B.H., et al: The multimodal brain tumor image segmentation benchmark (brats). *IEEE transactions on medical imaging* **34**(10), 1993–2024 (2014)
2. Sekuboyina, A., et al: Verse: a vertebrae labelling and segmentation benchmark. *arXiv preprint arXiv:2001.09193* (2020)
3. Bilic, P., et al: The liver tumor segmentation benchmark (lits). *arXiv preprint arXiv:1901.04056* (2019)
4. Bakas, S., et al: Identifying the best machine learning algorithms for brain tumor segmentation, progression assessment, and overall survival prediction in the brats challenge. *arXiv preprint arXiv:1811.02629* (2018)
5. Ronneberger, O., et al: U-net: Convolutional networks for biomedical image segmentation. In: *International Conference on Medical image computing and computer-assisted intervention*. pp. 234–241. Springer (2015)
6. Weller, M., et al: Eano guideline for the diagnosis and treatment of anaplastic gliomas and glioblastoma. *The lancet oncology* **15**(9), e395–e403 (2014)
7. Wen, P.Y., et al: Updated response assessment criteria for high-grade gliomas: response assessment in neuro-oncology working group. *Journal of clinical oncology* **28**(11), 1963–1972 (2010)
8. Maier-Hein, L., et al: Why rankings of biomedical image analysis competitions should be interpreted with care. *Nature communications* **9**(1), 1–13 (2018)
9. Taha, A.A., Hanbury, A.: Metrics for evaluating 3d medical image segmentation: analysis, selection, and tool. *BMC medical imaging* **15**(1), 1–28 (2015)
10. Hashemi, S.R., et al: Asymmetric loss functions and deep densely-connected networks for highly-imbalanced medical image segmentation: Application to multiple sclerosis lesion detection. *IEEE Access* **7**, 1721–1735 (2018)
11. Milletari, F., et al: V-net: Fully convolutional neural networks for volumetric medical image segmentation. In: *2016 fourth international conference on 3D vision (3DV)*. pp. 565–571. IEEE (2016)
12. Sudre, C.H., et al: Generalised dice overlap as a deep learning loss function for highly unbalanced segmentations. In: *Deep learning in medical image analysis and multimodal learning for clinical decision support*, pp. 240–248. Springer (2017)
13. Rahman, M.A., Wang, Y.: Optimizing intersection-over-union in deep neural networks for image segmentation. In: *International symposium on visual computing*. pp. 234–244. Springer (2016)
14. Brosch, T., et al: Deep convolutional encoder networks for multiple sclerosis lesion segmentation. In: *International conference on medical image computing and computer-assisted intervention*. pp. 3–11. Springer (2015)

15. Salehi, S.S.M., et al: Tversky loss function for image segmentation using 3d fully convolutional deep networks. In: International workshop on machine learning in medical imaging. pp. 379–387. Springer (2017)
16. Karimi, D., Salcudean, S.E.: Reducing the hausdorff distance in medical image segmentation with convolutional neural networks. *IEEE Transactions on medical imaging* **39**(2), 499–513 (2019)
17. Zhao, Y.X., et al: Multi-view semi-supervised 3d whole brain segmentation with a self-ensemble network. In: International Conference on Medical Image Computing and Computer-Assisted Intervention. pp. 256–265. Springer (2019)
18. Langerak, T.R., et al.: Label fusion in atlas-based segmentation using a selective and iterative method for performance level estimation (simple). *IEEE transactions on medical imaging* **29**(12), 2000–2008 (2010)
19. Feng, X., Tustison, N., Meyer, C.: Brain tumor segmentation using an ensemble of 3d u-nets and overall survival prediction using radiomic features. In: Crimi, A., Bakas, S., Kuijf, H., Keyvan, F., Reyes, M., van Walsum, T. (eds.) International MICCAI Brainlesion Workshop. pp. 279–288. Springer, Cham (2019)
20. Isensee, F., et al: No new-net. In: International MICCAI Brainlesion Workshop. pp. 234–244. Springer, Cham (2019)
21. McKinley, R., Meier, R., Wiest, R.: Ensembles of densely-connected cnns with label-uncertainty for brain tumor segmentation. In: Crimi, A., Bakas, S., Kuijf, H., Keyvan, F., Reyes, M., van Walsum, T. (eds.) International MICCAI Brainlesion Workshop. pp. 456–465. Springer, Cham (2019)
22. Weninger, L., Rippel, O., Koppers, S., Merhof, D.: Segmentation of brain tumors and patient survival prediction: Methods for the brats 2018 challenge. In: Crimi, A., Bakas, S., Kuijf, H., Keyvan, F., Reyes, M., van Walsum, T. (eds.) International MICCAI Brainlesion Workshop. pp. 3–12. Springer, Cham (2019)
23. Marcinkiewicz, M.e.a.: Segmenting brain tumors from mri using cascaded multi-modal u-nets. In: International MICCAI Brainlesion Workshop. pp. 13–24. Springer, Cham (2019)
24. Nuechterlein, N., Mehta, S.: 3d-espnet with pyramidal refinement for volumetric brain tumor image segmentation. In: Crimi, A., Bakas, S., Kuijf, H., Keyvan, F., Reyes, M., van Walsum, T. (eds.) International MICCAI Brainlesion Workshop. pp. 245–253. Springer, Cham (2019)
25. Kofler, F., et al: Brats toolkit: Translating brats brain tumor segmentation algorithms into clinical and scientific practice. *Frontiers in neuroscience* **14** (2020)
26. De Leeuw, J.R.: jspsych: A javascript library for creating behavioral experiments in a web browser. *Behavior research methods* **47**(1), 1–12 (2015)
27. Jungo, A., et al: pymia: A python package for data handling and evaluation in deep learning-based medical image analysis. *Computer methods and programs in biomedicine* **198**, 105796 (2021)
28. Drozdal, M., et al: The importance of skip connections in biomedical image segmentation. In: Deep learning and data labeling for medical applications, pp. 179–187. Springer (2016)
29. Bates, D., et al: Fitting linear mixed-effects models using lme4. *Journal of Statistical Software* **67**(1), 1–48 (2015). <https://doi.org/10.18637/jss.v067.i01>
30. Nakagawa, S., et al: The coefficient of determination r^2 and intra-class correlation coefficient from generalized linear mixed-effects models revisited and expanded. *Journal of the Royal Society Interface* **14**(134), 20170213 (2017)
31. Isensee, F., et al: nnu-net: a self-configuring method for deep learning-based biomedical image segmentation. *Nature Methods* **18**(2), 203–211 (2021)

32. Isensee, F., et al: nnu-net for brain tumor segmentation. arXiv preprint arXiv:2011.00848 (2020)
33. Reinke, A., et al: How to exploit weaknesses in biomedical challenge design and organization. In: Medical Image Computing and Computer Assisted Intervention – MICCAI 2018. pp. 388–395. Springer, Cham (2018)
34. Wagemans, J., et al: A century of gestalt psychology in visual perception: I. perceptual grouping and figure–ground organization. Psychological bulletin **138**(6), 1172 (2012)
35. Roelfsema, P.R.: Cortical algorithms for perceptual grouping. Annu. Rev. Neurosci. **29**, 203–227 (2006)
36. Wong, B.: Points of view: Color blindness. Nature Methods **8**(6), 441 (2011)

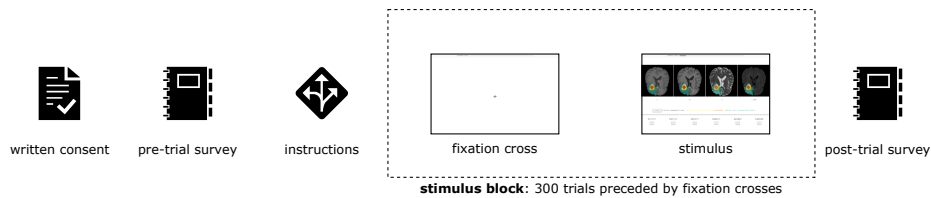


Fig. 7. Sequence of the experiments from left to right. Participants were instructed to conduct the evaluations in a suitable environment for reading MR exams. The experiment started with participants declaring consent. After this participants answered a survey with questions regarding their age, gender and various items to measure their experience with glioma segmentation. After that 300 trials were presented in random sequence to account for order effects. At the end we implemented a short post-trial survey, where doctors could provide feedback. Figure 1 illustrates a trial. All stimuli were presented on a neutral-grey background. Colorful items like the segmentation labels used a color-blind friendly color palette [36]. Besides the answers to our questionnaires and the segmentation quality assignment we recorded how often participants toggled the display of the segmentation labels and reaction times. Participants could toggle the display of the semi-opaque segmentation labels by pressing the spacebar. The star rating was assigned by pressing the corresponding key on the keyboard. The hotkeys were selected accounting for several international keyboard layouts and in order to minimize and equalize reaction times. Following assignment of a rating the experiment automatically progressed to presentation of the next trial. A fixation-cross was presented in the inter-trial-interval (ITI) which was displayed for a quasi random duration of 125 / 250 / 500 / 750 milliseconds so participants could not anticipate the start of subsequent trials. To allow for recording of accurate reaction times the experiment was realized using *JS Psych v6.1* [26] embedded into a *Vue JS v2.6* web application.

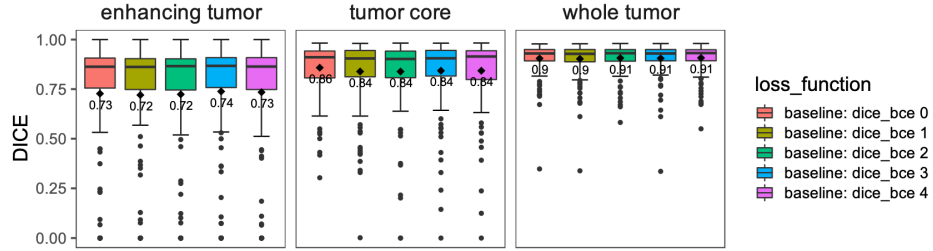


Fig. 8. Illustration of training variance. Diamonds indicate mean scores. To get an estimate of the randomness involved in our training process we trained our *nnU-net* implementation five times with *DICE+BCE* loss. We observe a dice performance between 0.72 and 0.74 , which is lower than the performance of our loss candidates.

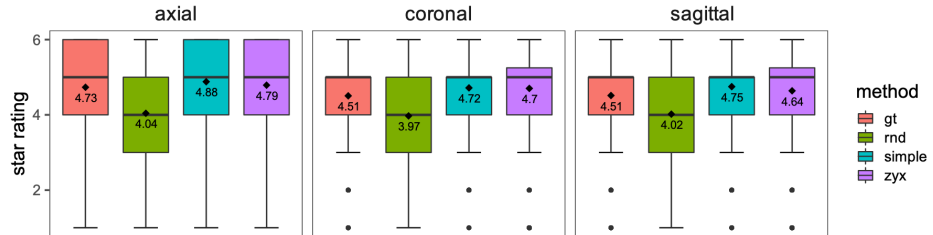


Fig. 9. Star rating across views. Diamonds indicate mean scores. The distribution is constant per *axial*, *coronal* and *sagittal* view. In general, segmentation quality ratings seem slightly higher on the axial view. We speculate this might occur because doctors usually annotate on the axial view, so the resulting annotation quality should be slightly higher. In addition, the resolution is often higher in the axial plane leading to less ambiguity when judging the quality of segmentation images.

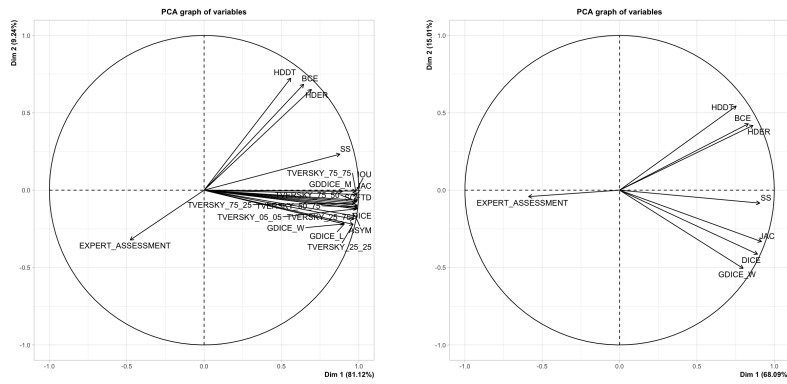


Fig. 10. PCA analysis with two factors. The scree plot and multiple non graphical tests show that two factors are sufficient to describe the loss landscape. PCA analysis with the full set of loss functions on the *left*, for the sake of clarity we repeated the PCA analysis with a subset of commonly used loss functions on the *right*. Similar to the hierachical clustering one can see how expert assesment can be described as combination of two factors. While the volumetric losses load mainly on dimension one, only *BCE* and the two Hausdorff losses cover dimension two. This might explain why the empirically found baseline *DICE+BCE* performs well across many segmentation tasks.